Design of 4-layered structure with single Cr-W alloy layer to achieve high and broadband photon-to-heat conversion efficiency

YAO Yuan[1], HU Er-Tao[2], ZANG Kai-Yan[1], ZHANG Jing-Ru[1], TU Hua-Tian[1], WEI Wei[2], WANG Song-You[1], ZHAO Hai-Bin[1], ZHENG Yu-Xiang[1], CHEN Liang-Yao[1]*

(1. Department of Optical Science & Engineering, Fudan University, Shanghai 200433, China；
2. School of O&E Eng., Nanjing University of Posts and Telecommunications, Nanjing 210023, China)

Abstract：A composition dependent model based on the Cr-W alloy structure has been studied to make it possible to be put into practical application. In terms of the optical properties of the Cr-W alloy with defined composition, a simpler 4-layered structure with single Cr-W alloy absorption layer has been designed to show the merit of high photon-to-heat conversion efficiency in the broad spectral region of 300 ~ 1 000 nm.

Key words：Cr-W alloy, optical model of alloy, photon-to-heat conversion film structure

PACS：71. 20. Be, 78. 20. nb, 78. 20. Bh

运用铬钨合金提升四层膜系结构的宽光谱光热转换效率

姚　远[1]，胡二涛[2]，臧恺岩[1]，张静如[1]，涂华恬[1]，韦　玮[2]，王松有[1]，赵海斌[1]，郑玉祥[1]，陈良尧[1]*
(1. 复旦大学 光科系，上海　200433；
2. 南京邮电大学 光电工程学院，江苏 南京　210023)

摘要：基于铬钨合金能带结构的研究,得到了可表述任意铬钨合金组分光学性质的数学模型,并将其应用于实际光热器件特性分析. 根据由模型获得特定组分铬钨合金的光学性质,设计了一个含有单层铬钨合金吸收层的四层膜结构,显示出优异的宽光谱(300 ~ 1 000 nm)光热转换性能.

关　键　词：铬钨合金；合金光学模型；光热转换薄膜

中图分类号：O43　　**文献标识码**：A

Introduction

In past years, the research had been carried out to focus on photon-to-heat conversion based on the multilayer film structure to achieve high photon energy absorption in a broad wavelength region. In 2007, we proposed and tested a 4-layer metal/dielectric film structure using Ti as the absorption layer[1], which achieved a photon-to-heat conversion rate of > 95% in the 400 ~ 700 nm spectra range.

To improve its performance, we tried many other materials and different structures. The performance of a 6-layer film structure, designed in 2013, was significantly improved in the UV region[2]. Another design, using an 8-layer structure, the high absorption region even can be extended to the 250 ~ 2 000 nm wavelength region.

In those studies, with the most known materials applied in the data simulation and test, we found that a much more complicated structure will be required to improve more of the performance of the device. From 4-layer structure to the newly designed 8-layer structure, we can only achieve better performance with the cost of a much-complicated structure, which results in higher cost and complex fabrication process to make it be less feasible in the application. In this case, a new approach to find the material with proper optical properties will be required to improve the performance without adding more layers to the structure.

In this work, an analytical model of the Cr-W alloy material has been studied to make it possible that any Cr-W alloy with the new optical property that is different

from the ones owned by the individual element material can be acted as the absorption and reflection layer in the simpler 4-layer film structure. This certainly can provide us with a new method for the design of the multilayer film structure.

1 Dielectric function model

Usually, the optical property of new materials has to be tested before we can design a multilayer structure with it. This may cost a lot of work trying to find out what composition of the alloy to be best for a film structure, especially when there are more than one alloy layers required in the structure.

An analytical model of Cr-W alloy will enable us to predict the optical property with a certain composition. With the help of this model, a simple optimization procedure will produce a solution with the best composition of the alloy for the structure.

Rioux et al. had proposed an analytical dielectric model of Au-Ag alloy based on critical point analysis of the band structure[3]. They fitted the model to extract the values of dielectric function ε for Au, Ag, and AuAg50: 50, respectively. We will use the same method to establish the dielectric model for Cr, W, and their alloys.

Most of the inflections occurred in the dielectric function are correlated to the critical points (Van Hove singularities)[4] of the joint density of states (jDOS). According to the work by Rioux et al, due to the critical point attributed by the interband transitions, the dielectric function ϵ_{ib} can be presented as a convolution of jDOS and a Lorentz oscillator[5]:

$$\epsilon_{ib}(\omega) = A \int_0^\infty \frac{jDOS(\omega_{lK})}{\omega_{lK}(\omega_{lK}^2 - (\omega + i\Gamma)^2)} \quad , (1)$$

where A is the amplitude parameter, k and l in frequency ω_{lk} are the occupied and empty states, respectively, and $\hbar\omega_{lk}$ is the transition energy between these two states. Thus, the model of jDOS in Eq. 1 is required to obtain the dielectric function of ε.

The function of jDOS is mainly affected by the characteristic of critical points in the Brillouin zone, most of which are located at the high symmetry point of the band structure. The band structure of Cr and W around high symmetry points is calculated by using the CASTEP approach based on density functional theory with the result shown in Fig. 1.

Both W and Cr crystals have a body-centered cubic (BCC) symmetry with the middle point K along the Δ (Γ-H) line. At the Γ symmetry point of W, there are two different types of critical points with the same transition energy of 3.5 eV: an M0 type with positive effective mass along three directions (all three directions are along the Γ-H line in this case due to symmetry) and an M3 type with negative effective mass along three directions in the same situation. At the N symmetry point of W, the critical point is the M3 type (two directions are along the N-P line due to symmetry, and another is along the N-K line in this case). According to the work by Christensen et al[6], there is another M2 critical point along the Σ (Γ-N) line near the middle point with transition energy around 3 eV.
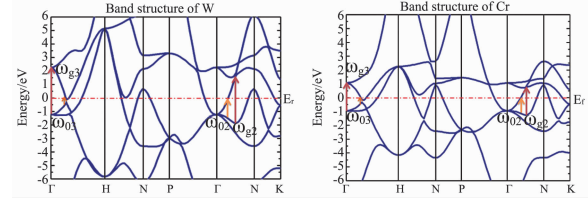

Fig. 1 The band structure of W and Cr around the M2 critical point along the Σ line near the middle point and the M3 critical point at the Γ symmetry point

图 1 W 和 Cr 在 M2 临界点（Σ 方向上 Γ 及 N 高对称点中点位置），以及 M3 临界点（在 Γ 高对称点上）附近的能带结构示意图

Preliminary fits show that in the 0.5 ~ 5.1 eV region, the dielectric function of both W and Cr are mainly affected by the M2 critical point along the Σ line near the middle point and the M3 critical point at the Γ symmetry point.

The function of jDOS near the M2 critical point can be approximated by a parabolic expansion:

$$jDOS(\omega) \propto \begin{cases} C_2 & (\omega < \omega_{g2}) \\ C_2 - \sqrt{\omega - \omega_{g2}} & (\omega > \omega_{g2}) \end{cases}$$
$$(2)$$

At any energy lower than ω_{02} shown in Fig. 2, the jDOS will be zero. Then the contribution to ε in Eq. 1 will become:

$$\epsilon_{CP2}(\omega) =$$
$$A_2 \left[\int_{\omega_{g2}}^\infty \frac{C_2 \cdot d\omega_{lk}}{\omega_{lk}(\omega_{lk}^2 - (\omega + i\Gamma_2)^2)} - \int_{\omega_{g2}}^\infty \frac{\sqrt{\omega_{lk} - \omega_{g2}}}{\omega_{lk}(\omega_{lk}^2 - (\omega + i\Gamma_2)^2)} d\omega_{lk} \right]$$
$$= \frac{-A_2}{2(\omega + i\Gamma_2)^2} \left[C_2 \ln\left(1 - \left(\frac{\omega + i\Gamma_2}{\omega_{02}}\right)^2\right) + \pi(2\sqrt{\omega_{g2}} - \sqrt{\omega_{g2} + \omega + i\Gamma_2}) - \sqrt{\omega_{g2} - \omega - i\Gamma_2} \right] \quad (3)$$

For an M3 critical point, the jDOS is:

$$jDOS(\omega) \propto \begin{cases} C_3 + \sqrt{\omega_{g3} - \omega} & (\omega < \omega_{g3}) \\ C_3 & (\omega > \omega_{g3}) \end{cases} \quad (4)$$

At any energy lower than ω_{03} in Fig. 2, the jDOS is zero. By letting $jDOS(\omega_{03}) = 0$ in Equation 4, we have: $C_3 = -\sqrt{\omega_{g3} - \omega_{03}}$. The contribution of the M3 critical point is then:

$$\epsilon_{CP3}(\omega) =$$
$$A_3 \left[\int_{\omega_0}^\infty \frac{C_3 \cdot d\omega_{lk}}{\omega_{lk}(\omega_{lk}^2 - (\omega + i\Gamma_3)^2)} + \int_{\omega_{03}}^{\omega_{g3}} \frac{\sqrt{\omega_{g3} - \omega_{lk}} \cdot d\omega_{lk}}{\omega_{lk}(\omega_{lk}^2 - (\omega + i\Gamma_3)^2)} \right]$$
$$= A_3 \left[-\frac{C_3}{2(\omega + i\Gamma_3)^2} \ln\left(1 - \left(\frac{\omega + i\Gamma_3}{\omega_{03}}\right)^2\right) - \frac{2\sqrt{\omega_{g3}}}{(\omega + i\Gamma_3)^2} \tanh^{-1}\right.$$
$$\left(\sqrt{\frac{\omega_{g3} - \omega_{03}}{\omega_{03}}}\right) + \frac{\sqrt{\omega + i\Gamma_3 - \omega_{g3}}}{(\omega + i\Gamma_3)^2} \tan^{-1}\left(\sqrt{\frac{\omega_{g3} - \omega_{03}}{\omega + i\Gamma_3 - \omega_{g3}}}\right)$$
$$\left. + \frac{\sqrt{\omega + i\Gamma_3 + \omega_{g3}}}{(\omega + i\Gamma_3)^2} \tanh^{-1}\left(\sqrt{\frac{\omega_{g3} - \omega_{03}}{\omega + i\Gamma_3 + \omega_{g3}}}\right) \right] \quad (5)$$

Here we use $J = A \cdot C$ and $K = 1/C$ instead of A and C for the convenience of setting the parameter range. Since the jDOS of W has an M2 and an M3 type critical point, the dielectric function can be written as an equation with 13 parameters all being defined previously:

$$\varepsilon_W(\omega) = \varepsilon_\infty - \frac{\omega_p^2}{\omega^2 + i\omega\Gamma_p} + \epsilon_{CP2}(\omega, A_2, C_2, \omega_{g2}, \Gamma_2)s1$$
$$+ \epsilon_{CP3}(\omega, A_3, C_3, \omega_{g3}, \omega_{03}, \Gamma_3)$$
$$= \varepsilon_\infty - \frac{\omega_p^2}{\omega^2 + i\omega\Gamma_p} + \epsilon_{CP2}(\omega, J_2, K_2, \omega_{g2}, \Gamma_2) +$$
$$\epsilon_{CP3}(\omega, J_3, K_3, \omega_{g3}, \omega_{03}, \Gamma_3) \quad . \quad (6)$$

The dielectric function of Cr and Cr-W alloy with different composition has exactly the same form of Eq. 6. Parabolic approximates are used to model each parameter. 3 groups of the sub-parameters have been achieved by fitting the model to the measured ε of different composition. Thus, each parameter in the composition dependent model of Cr-W alloy can be described by a composition function defined by 3 groups of sub-parameters. For example, the plasmonic frequency ω_p with a tungsten molar fraction (WMF) can be calculated using the equation:

$$\omega_p(WMF) = \alpha(WMF)^2 + bWMF + c . \quad (7)$$

After all the binomial coefficient of 13 parameters determined by fitting, the complete model of Cr-W alloy of arbitrary composition is defined only by WMF, to make it possible design and optimize a multilayer structure using the Cr-W alloy as the absorption and reflection layer.

2　Measurement result

Figure 2 shows the real and imaginary parts of ε for the six measured films. All six metal and alloy films deposited by the magnetron sputtering method are thicker than 250 nm. The transition is much sharper for the pure metals comparing with the alloys, which is in agreement with the results in Au-Ag alloys[3].

3　Fitting procedure

A genetic algorithm is used in the data fitting procedure[7-8]. This method forms a generation containing 13 parameters. For the first generation, the value is randomly chosen for each parameter. The fitness of each individual parameter in the generation is determined by the least variance between the measured and modeled dielectric function. The individual parameter with higher fitness has a higher probability to undergo to the next round of reproduction. With enough generations, the best fitted parameters will be generated to present the data in consistency with the measured ones.

Table 1 shows the fitting parameters for the dielectric function of Cr-W alloy. Figure 3 shows the real and imaginary parts of measured dielectric function of CrW 57:43 and the one predicted by the model which is in good agreement with the experimentally measured ones.

Fig. 2　Measured a）real and b）imaginary parts of the dielectric function ε for Cr, W and Cr-W alloy
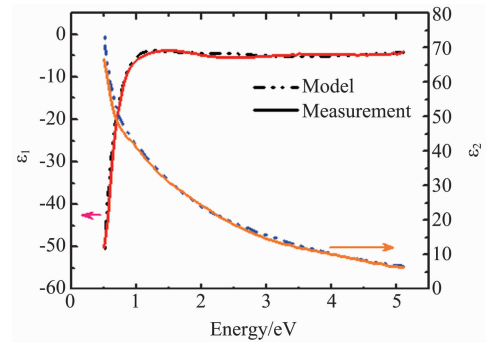图 2　Cr, W 以及 Cr-W 合金介电函数 ε 的测量结果（a）实部，（b）虚部

Fig. 3　Modeled（dashed lines）and measured（solid lines）dielectric function for CrW 57:43
图 3　CrW 57:43 介电函数的模型计算结果（虚线）以及测量结果（实线）

表 1　Fitting parameters for the dielectric function of Cr-W alloy
表 1　Cr-W 合金介电函数的拟合参数

	ω_p/eV	Γ_p	ε_∞/eV	ω_{g2}/eV	ω_{02}/eV	Γ_2	J_2	K_2	ω_{g3}/eV	ω_{03}/eV	Γ_3	J_3	K_3
W	5.927	0.133	1.585	2.403	2.395	0.999	103.873	0.301	2.228	0.475	0.991	37.323	0.271
CrW48:52	5.481	0.205	0.918	2.412	2.390	0.998	62.958	0.287	2.324	0.329	0.998	44.644	0.725
Cr	5.546	0.395	2.599	2.876	1.653	0.542	39.533	0.995	1.789	0.611	0.683	49.198	0.620

4　Multilayer structure

The photon-to-heat conversion multilayer structure was designed and simulated using the transmission matrix method[9-11].

After choosing material for each layer, the thickness of these layers is set as the optimal variable. In most cases, the structure with more layers will be required with the thickness variable being optimally adjusted to get the best result.

However, the structure with more layers also will lead to the fabrication process in a more complicated way with higher cost to be less favorable for application. Here we use the composition of the alloys as the variable to perform the optimal calculation by replacing the pure metal with alloys instead of adding the additional layers into the structure.

The sketch of newly designed 4-layer structure is shown in Fig. 4. From top to bottom, we use a layer of SiO_2 (~ 100 nm) as protection and antireflection layer; the Cr-W alloy layer (5 ~ 15 nm) to play a key role for photon energy absorption; another SiO_2 layer (~ 100 nm) is responsible for phase matching. At the bottom we also use Cr-W alloy layer (> 200 nm) as a high reflection layer to avoid any light penetration through the structure.
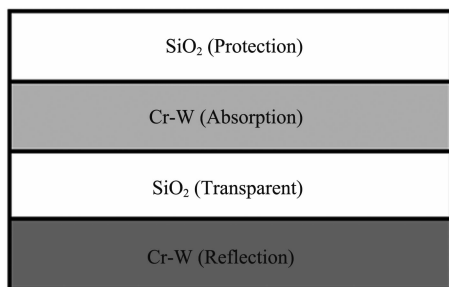

| SiO₂ (Protection) |
| Cr-W (Absorption) |
| SiO₂ (Transparent) |
| Cr-W (Reflection) |

Fig. 4　Schematic structure of newly designed 4-layer alloy/dielectric device consisting of [SiO_2/Cr-W/SiO_2/Cr-W]

图4　新设计的四层合金/介质多层膜系结构示意图 [SiO_2/Cr-W/SiO_2/Cr-W]

The optimizing procedure also uses a genetic algorithm. The variable values, including the thickness and the composition (WMF) of the Cr-W alloy, initially are randomly chosen for each layer. The best fitness is obtained by taking the largest photon-to-heat conversion rate in the spectral region of 300 ~ 2 000 nm considering the weight of AM 1. 5 solar spectrum[2,12]. The absorption spectra of the simulated structure [SiO_2 90. 7 nm/Cr 5. 2 nm/SiO_2 93. 4 nm/ CrW33:67 >200 nm] is shown in Fig. 5 with comparison to the absorption spectra of early designed 4-layer and 6-layer structures. The calculated conversion rate of the simpler 4-layer structure using CrW 33:67 as the reflection layer is 96. 38%, better than 92. 85% of the 4-layer structure using the pure Ti metal, close to 99. 45% of the 6-layer structure.

The reflection of the sample is tested by a spectrophotometer. As the transmission of the structure is zero, the absorption can be calculated by equation：$A = 1 - R$.

The measured absorption is shown in Fig. 6 with a conversion rate in average of 93. 87%. The SEM image is shown in Fig. 7.
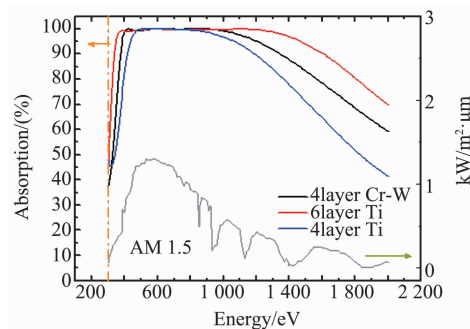

Fig. 5　Black line is the simulated absorption spectrum for 4-layer structure [SiO_2 90. 7 nm/Cr 5. 2 nm/SiO_2 93. 4 nm/ CrW33:67 >200 nm]. The absorption spectra of the early designed 4 and 6-layer structures are also presented in comparison

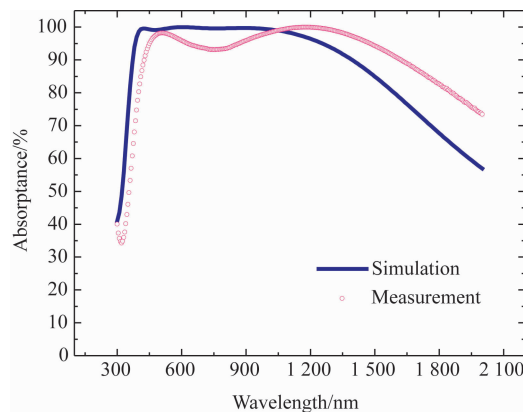图5　图中黑线为四层膜结构 [SiO_2 90. 7 nm/Cr 5. 2 nm/ SiO_2 93. 4 nm/ CrW33:67 >200 nm]吸收谱线的模拟结果. 蓝线及红线分别为过往的四层及六层膜系设计的测量结果

Fig. 6　Tested and calculated absorption of newly designed 4-layer alloy/dielectric device consisting of [SiO_2/Cr /SiO_2/ CrW 33:67]

图6　四层合金/介质膜结构吸收谱线的测量结果与计算结果对比. 器件结构为：[SiO_2/Cr /SiO_2/CrW 33:67]

5　Conclusion

We have built a model to establish the dielectric function of Cr-W alloys with variable composition and applied it for design of a 4-layer photon-to-heat conversion structure.

The new design using CrW 33:67 alloy as the reflection layer to achieve a 93. 87% photon-to-heat conversion rate in 300 ~ 2 000 nm range with the simpler 4-layer structure, showing a good prospect of the application of the alloy in the design of multilayer films.

Experiment section
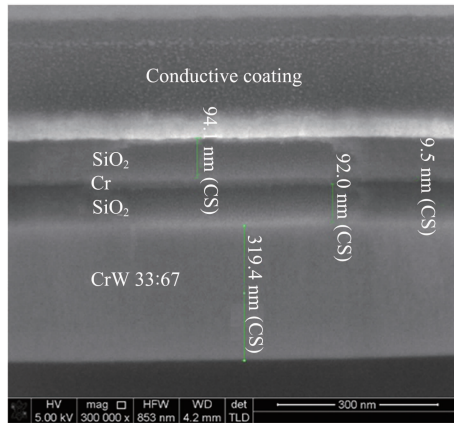
Magnetron Sputtering：Alloy thin films are deposited

Fig. 7　SEM image shows clearly the 4-layer structure. The thickness of each layer is about：［SiO₂ 94. 1nm/Cr 9. 5nm/ SiO₂ 92. 0 nm/ CrW33：67 319. 4 nm］. The thickness of Cr layer is hard to judge due to the transition layer between Cr and SiO₂ layer

图 7　SEM 图像下可见清晰的四层膜结构. 各层膜层厚度为：［SiO₂ 94. nm/Cr 9. 5nm/SiO₂ 92. nm/ CrW33：67 319 nm］. 由于 Cr 和 SiO₂ 层之间存在过渡层使得 Cr 层的厚度从图中较为难以辨认

by co-sputtering Cr and W on the 1. 2 mm-thick Si wafer using INFOVION ISB-1200 magnetron sputtering system. The working pressure is 1 mtorr.

Composition of each sample is analyzed by ICP-AES method，using Jarrell-Ash Atom Scan 2 000. Dielectric function is measured by the ellipsometry method using a Wollam-VASE ellipsometer. The absorption spectrum of the 4-layer structure was tested by a SHIMADZU UV3600PLUS spectrophotometer.

Acknowledgment

References

［1］Miao J，Chen L Y，Zhou P，*et al*. High solar absorption of a multilayered thin film structure［J］. *Optics Express*，2007，**15**（4）：1907 − 1912.

［2］Liu M H，Hu E T，Yao Y，*et al*. High efficiency of photon-to-heat conversion with a 6-layered metal/dielectric film structure in the 250 ~ 1 200 nm wavelength region.［J］. *Optics Express*，2014，22 Suppl 7（S7）：A1843.

［3］Rioux D，Vallières S，Besner S，*et al*. an analytic model for the dielectric function of Au，Ag，and their alloys［J］. *Advanced Optical Materials*，2014，**2**（2）：176 − 182.

［4］Van Hove L. The occurrence of singularities in the elastic frequency distribution of a crystal［J］. *Physical Review*，1953，**89**（6）：1189 − 1193.

［5］Cardona M. *Modulation spectroscopy*［M］. Academic Press，1969.

［6］Christensen N E，Feuerbacher B. Volume and surface photoemission from tungsten. I. Calculation of band structure and emission spectra［J］. *Physical Review B Condensed Matter*，1974，**10**（6）：2349 − 2372.

［7］Mitchell M. *An Introduction to Genetic Algorithms*［M］. MIT Press，CambridgeDBLP，1998.

［8］Coello C A C，Christiansen A D，Aguirre A H. *Automated Design of Combinational Logic Circuits by Genetic Algorithms*［M］// Artificial Neural Nets and Genetic Algorithms. Springer Vienna，1998：333 − 336.

［9］Behrman D. *Routledge revivals*：*Solar energy*［M］. Routledge，1976.

［10］Seraphin B O. Solar energy conversion：Solid-state physics aspects［J］. 1979，**5**（4206）：852 − 856.

［11］Sergeant N P，Pincon O，Agrawal M，*et al*. Design of wide-angle solar-selective absorbers using aperiodic metal-dielectric stacks［J］. *Optics Express*，2009，**17**（25）：22800 − 12.

［12］Bermel P，Lee J，Joannopoulos J D，*et al*. Selective solar absorbers［J］. *Research Gate*，2012，**15**（15）：231 − 254.